Ibn Al-Haitham Journal for Pure and Applied Sciences
Journal homepage: jih.uobaghdad.edu.iq
PISSN: 1609-4042, EISSN: 2521-3407
IHJPAS. 2025, 38(3)

Sensing and Magnetic Properties in Zn-$CdFe_2O_4$ Spinel Ferrite Doped with SnO_2 Prepared by Sol-Gel Auto Combustion

Mariam O. Abd Alkareem[1] and Tagreed M. Al-Saadi[2*]
[1,2] Department of Physics, College of Education for Pure Sciences (Ibn Al-Haitham), University of Baghdad, Baghdad, Iraq.
*Corresponding Author.

Received: 30 January 2024 Accepted: 23 April 2025 Published: 20 July 2025
doi.org/10.30526/38.3.40788

Abstract

The sol-gel method was used in this study to create the Zn-$CdFe_2O_4/SnO_{2(0.15)}$ nano ferrite, and XRD, FE-SEM, and EDX methods were used to evaluate the nano ferrite's characteristics. The findings showed that the lattice constant of the sample $CdFe_2O_4/SnO_{2(0.15)}$ is higher than that of $ZnFe_2O_4/SnO_{2(0.15)}$ and $Zn_{0.5}Cd_{0.5}Fe_2O_4/SnO_{2(0.15)}$ and that the resultant compound possesses a cubic spinel ferrite phase. The crystal size was on the nanoscale, according to Scherrer-Williamson Hall. Based on the FE-SEM images, it can be noticed its shape as semi-spherical or spherical; the presence of elements Zn, Cd, Fe, Sn, and O was confirmed by the EDX test. The gas sensing showed good sensitivity to NO_2 gas and a short response and recovery time (15.3 sec, 49.5 sec). The magnetic properties were calculated using a vibrating sample magnetometer, where soft magnetic behavior was shown for all samples. The novel zinc cadmium ferrite preparation is expected to find use in a wide range of products, including biomedical equipment, motors, sensors for high-density data storage devices, and magnetic recording devices.

Keywords: Zn-Cd ferrite, Doped SnO_2, NO_2 gas, Sensitivity, Recovery time, Magnetic properties.

1. Introduction

There is growing interest in discovering novel materials to create solid-state gas sensors with great performance. Semiconductor metal oxide sensors are a reliable and affordable substitute for conventional detection methods. MFe2O4 spinel-type oxide semiconductors are materials that are sensitive to reducing and oxidizing gases (1).

NO_2 is regarded as hazardous to both human health and the environment. Thus, the creation of sensors to identify NO_2 gas is crucial (2) Nowadays, scientists are focused on ferrite materials due to their special physical characteristics, such as their optical, electrical, and magnetic because of their many uses in devices with low and high permeability, ferrofluids, microwaves, high-density storage devices, and magnetic drug delivery, ferrites are being studied for their gas detecting capabilities. A mixture of iron and metal oxides is called ferrite. ferrite exhibits ferrimagnetic properties, high electrical resistance, and dielectric behavior. Ferrites were divided into four categories: granites, orthoferrites, spinels, and hexagonal. Large magnetocrystalline anisotropy, high Ms, high curie temperature, and Hc were among the several characteristics displayed by spinel ferrite (3,4). The ferrite's metal created a divalent bond. 32 Oxygen atoms make up the unit cell in the cubic structure of spinel ferrite, which is composed of closely packed oxygen atoms. A) tetrahedrally coordinated sites, which are covered by four oxygen atoms, and B) octahedrally coordinated sites, which are covered by six oxygen atoms, are the two kinds of sites between anions that have an FCC face-centered cube configuration (5). Ferrite nanoparticles have been synthesized by a variety of chemical processes. These techniques include sol-gel (6), chemical co-precipitation (7), and micromulsion (8).

Among these techniques, the sol-gel approach is frequently employed to create ferrite nanoparticles. The ratio of metal nitrates to fuel, speed, stirring duration, pH, and fuel can all have a significant impact on the size and characteristics of spinel ferrite nanoparticles (9). Mehrfar et al. synthesized spinel ferrite MFe_2O_4 (M=Cd, Zn, Co) nanoparticles using the sol-gel method. The impact of metal M on linalool gas sensing performance was examined, and the findings showed that nano-$CdFe_2O_4$ is a viable gas detection option suggesting its potential utility in sensor manufacturing (10). Rezlescu et.al generated some spinel ferrite by spontaneous combustion of sol-gel and their gas-sensing properties were investigated. It was found from this study that $ZnFe_2O_4$ is sensitive and selective to ethanol (11). The series ($Co_{0.2}$ $Zn_{0.8-x}$ Cd_x Fe_2O_4) with (x=0, 0.3, 0.6) was prepared by rapid spontaneous combustion method and heated for two hours to 800°C. Magnetism was measured using a vibrating sample magnetometer (VSM). The nanoparticles were found to be soft magnetic materials since the hysteresis loop was minimal (12). The current study investigates the effect of the nano ferrite compound Zn-$CdFe_2O_4/SnO_{2(0.15)}$ on structure, sensing to NO_2 gas, and magnetic properties.

2. Materials and Methods

Zn-$CdFe_2O_4/SnO_{2(0.15)}$ with a weight ratio of SnO_2 (0.15), **Table (1)** lists the masses of raw ingredients needed to prepare ferrite, which was made using the sol-gel process. The metal nitrates are weighed and then dissolved in tiny volumes of distilled water. Using a magnetic stirrer, this solution is mixed with citric acid to form a homogeneous mixture. Drops of ammonia are added after mixing to reach the pH (~7). For an hour, the solution is heated to 80°C while being constantly stirred. After that, the solution is left to evaporate and stays at this temperature until it gels. Following that, the temperature is raised even higher to 110°C. At this point, the gel begins to dry when the temperature reaches 120°C, and the dry gel begins to ignite. After obtaining the resultant ferrite, each sample's combustion products are allowed to cool before being calcined in an oven set at 600°Cfor two hours.

Table 1. The masses of raw materials to produce Zn-$CdFe_2O_4/SnO_{2(0.15)}$

Sample	Composition	Ferric Nitrate		Zinc Nitrate		cadmium Nitrate		Tin chloride		Citric acid	
		n	m(g)	n	m(g)	n	m(g)	w	m(g)	n	m(g)
M_1	$ZnFe_2O_4/SnO_{2(0.15)}$	2	32.32	1	11.8996	0	0	0.15	1.7849	3	23.056
M_2	$CdFe_2O_4/SnO_{2(0.15)}$	2	32.32	0	0	1	12.3392	0.15	1.8509	3	23.056
M_3	$Zn_{0.5}Cd_{0.5}Fe_2O_4/SnO_{2(0.15}$	2	32.32	0.5	5.9498	0.5	6.1696	0.15	1.8179	3	23.056

3. Results and Discussion

3.1. X-ray diffraction analysis

An X-ray diffraction (XRD) analysis was performed to determine the composition of the Zn-Cd Fe_2O_4/SnO_2 phase in the range ($20° \leq 2\theta \leq 80°$). A cubic spinel structure type FCC (13) with planes [(220), (311), (222), (400), (422), (511), (440) and (533)] is confirmed by the indexed x-ray diffraction patterns of $Zn_{0.5}Cd_{0.5}Fe_2O_4/SnO_2$ which are displayed in figure 1. The diffraction values agree with the card numbers (no.22-1012), and (no.22-1063).

Lattice parameters were calculated using (Match! software) and the Scherrer equation was used to get the mean crystallite size (14, 15).

$$D_{sh} = 0.9\lambda/\beta\cos\theta \qquad (1)$$

Where D is the crystallite size, λ is the X-ray wavelength (1.54 Å), β is the full width at half maximum and θ is the incidence angle.

The following equation's x-ray density must be calculated (16):

$$\rho=8M_w/N_A.\ a^3 \qquad (2)$$

Where (MW) is the molecular weight, (NA) is the number of the Avogadro and (a) is the lattice constant

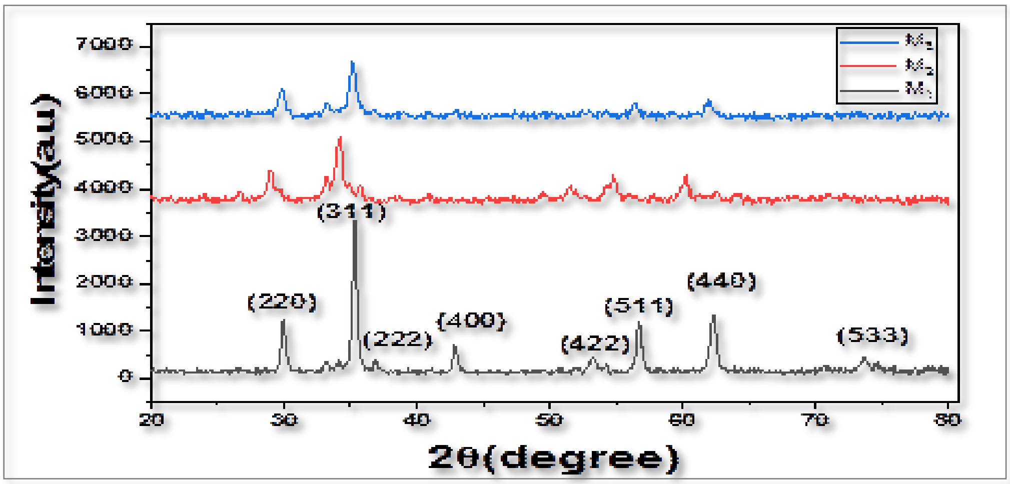

Figure 1. X-Ray diffraction of the Zn-$CdFe_2O_4/SnO_{2(0.15)}$ nano-ferrite.

Table (2) demonstrates that the $CdFe_2O_4/SnO_{2(0.15)}$ sample's lattice constant is greater than the $ZnFe_2O_4/SnO_{2(0.15)}$, $Zn_{0.5}Cd_{0.5}Fe_2O_4/SnO_{2(0.15)}$ sample's, the reason for this is that cadmium ionic radius(92pm) is greater than zinc ionic radius (47pm). The lattice constant rises when the cadmium ion enters the lattice or is positioned between host ions. This aligns with the researcher's findings (17) However, table2 illustrates that the crystallite size, as calculated by Scherrer equations, is at the nanoscale. We also used the Williamson-Hall to calculate the grain size (18,19)

$$\beta_{hkl} = (K\lambda/D) + 4\varepsilon \sin\theta \qquad (3)$$

where K: is constant, λ: is the Cu kα radiation wavelength, D: the average grain size, and ε: is the microstrain, the equation is plotted with sin θ on the x-axis and β cos θ on the y-axis for all samples to determine the average crystallite size and strain from the slope (the intercept Kλ/D and the 4ε) and y-axis intercept of the fitted line as shown in Figure 2 according to the Williamson-Hall, according to Table 2 , the microstrain for $ZnFe_2O_4/SnO_{2(0.15)}$, $Zn_{0.5}Cd_{0.5}Fe_2O_4/SnO_{2(0.15)}$ positive and for $CdFe_2O_4/SnO_{2(0.15)}$ is negative .This is explained by the fact that the transfer of iron ions between the octahedral and tetrahedral positions who created flaws in the magnetic nano oxide's structure that caused the sample's lattice to contract (20).

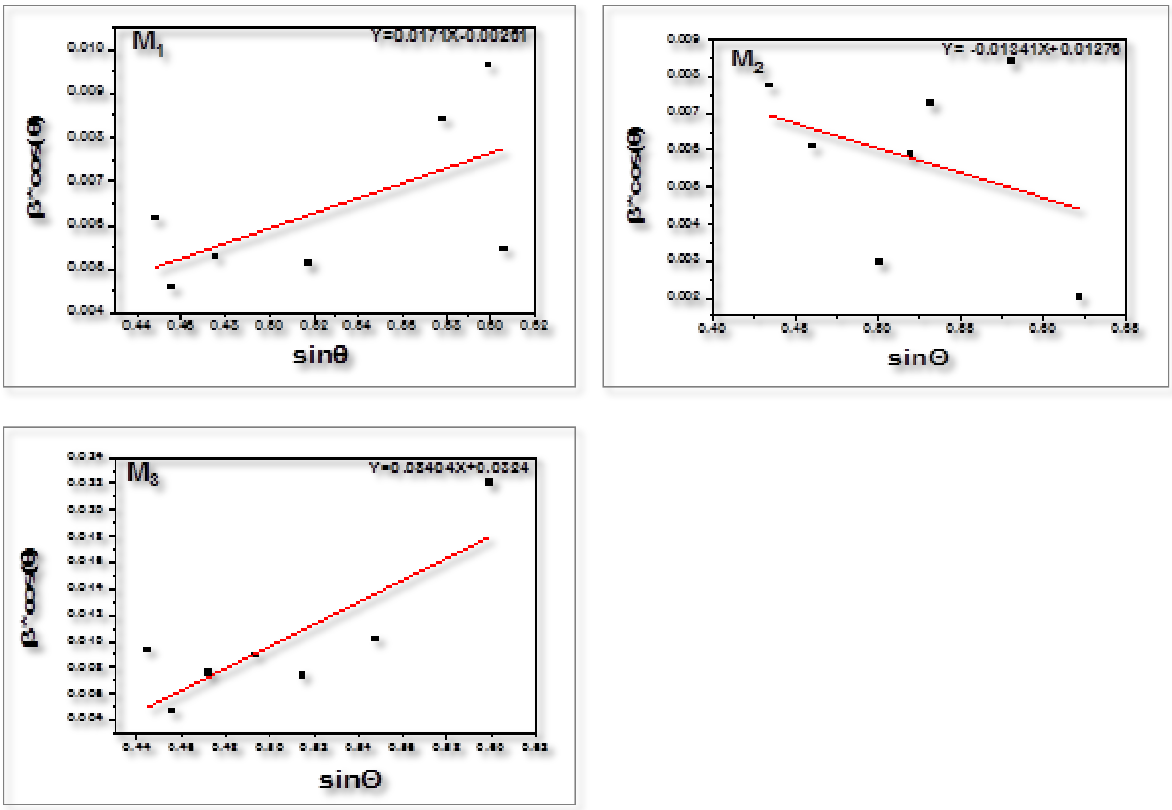

Figure 2. Williamson-Hall analysis of Zn-CdFe$_2$O$_4$/SnO$_{2(0.15)}$ nanoparticles.

Table 2. Lattice constants, crystallite size and density of Zn-CdFe$_2$O$_4$/SnO$_{2(0.15)}$ nano-ferrite.

samples	**Lattice constant (Å)**	**Density (g/cm^3)**	**D Sch. (nm)**	**D W-H (nm)**	**Microstrain ε * 10^{-3}**
M$_1$	8.4418	5.324	27.54	66.9	4.275
M$_2$	8.7003	6.249	28.33	10.8	-3.35
M$_3$	8.4926	6.108	26.46	4.27	2.101

3.2. Morphological analysis

The samples of the generated compound (Zn-CdFe$_2$O$_4$/SnO$_{2(0.15)}$) were photographed using the emission field scanning electron microscopy (FE-SEM) technique. It has been verified that the material is in the nanoscale region, as seen in **Figure (3),** it was observed that the particles had a spherical or semi-spherical form with some gaps and gatherings: this suggests that the compound is porous, which enhances the sensor's reaction to the gas (21).

3.3. Elemental analysis

EDX was used to analyze the samples produced using the auto-combustion process. The elements Fe, Zn, Cd, Sn, and O are represented by the observed peaks, which show that the Zn$_{0.5}$Cd$_{0.5}$Fe$_2$O$_4$/SnO$_{2(0.15)}$ sample's components have been examined in **Figure 4** EDX spectra. Demonstrating that the auto combustion (sol-gel) technique creates oxides with a high degree of elemental similarity (22, 23).

3.4. Sensing Properties

The powder was compressed at a pressure of 1.5t/cm^2 using a manual press. After that, the 1cm in diameter and 3.5 mm thick pellets were heated for two hours at 900°C. After that, they were automatically left to cool and heat in the oven. The electrodes for the samples were then made. The sensitivity of each sample to NO$_2$ gas across the specified temperature range (200°C, 250°C, and 300°C) was ascertained using gas sensitivity test equipment. At the concentration, the gas is 129.18pm (**Figure 5**).

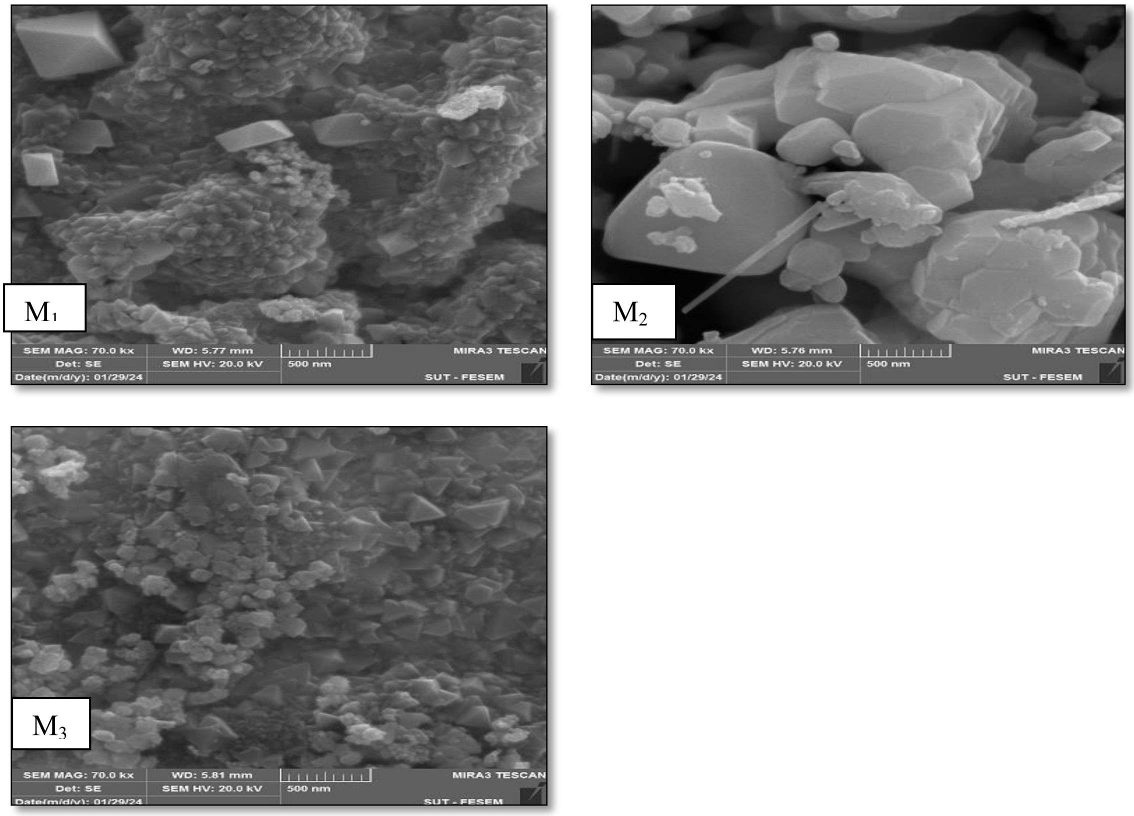

Figure 3. FE-SEM of Zn-$CdFe_2O_4/SnO_{2(0.15)}$ ferrite nanoparticles samples.

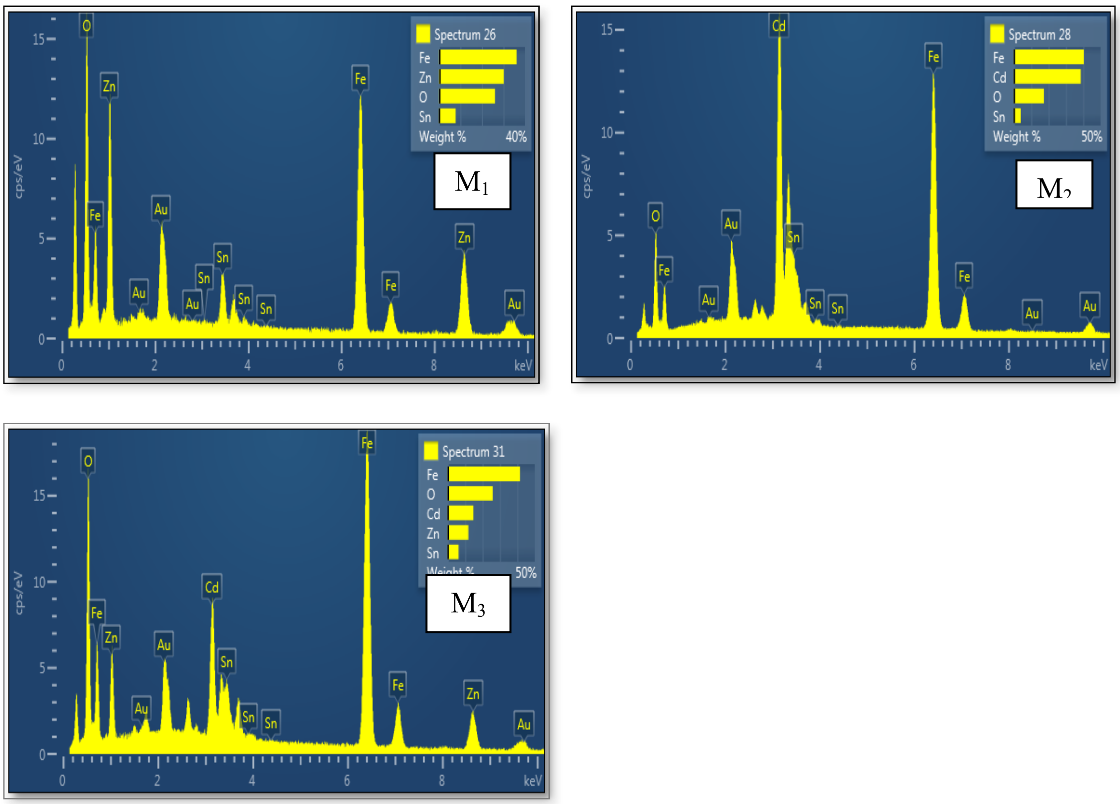

Figure 4. EDX of the nano ferrite samples Zn-$CdFe_2O_4/SnO_{2(0.15)}$

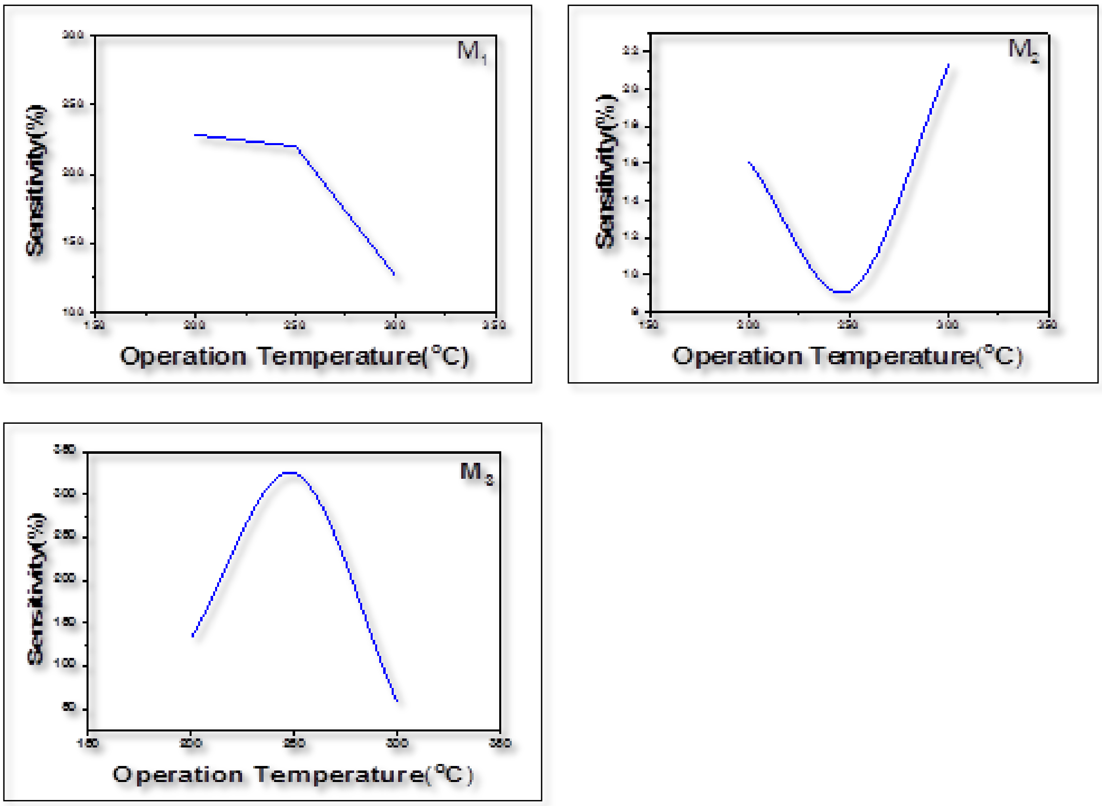

Figure 5. The relationship between sensitivity and operating temperature of Zn-$CdFe_2O_4/SnO_{2(0.15)}$

Table (3) shows the maximum sensitivity values for the Zn.$CdFe_2O_4/SnO_{2(0.15)}$ samples, and it is noteworthy that the maximum sensitivity value was at 250 °C.

Table 3. The highest sensitivity values of the NO_2 gas for Zn.$CdFe_2O_4/SnO_{2(0.15)}$ nanoparticles.

Samples	Operating Temperature	Highest sensitivity value (%)
M_1	200°C	228.409
M_2	300°C	21.315
M_3	250°C	324.390

The sensitivity of Zn-$CdFe_2O_4/SnO_{2(0.15)}$ samples to the oxidizing nitrogen gas (NO_2) was investigated, and it was found that all samples were sensitive to NO_2, enabling its usage in a variety of applications because of $Zn_{0.5}Cd_{0.5}Fe_2O_4/SnO_{2(0.15)}$ combination contains zinc, cadmium, and tin together, it has the lowest particle size, as seen in **Table (2)**, and it can find that it had the best sensitivity at 250°C. Therefore, a tiny particle size is linked to a compound's higher sensitivity (24). The tin element can improve the distribution of pore sizes, specific surface area, and porosity. More surface area indicates more active sites for NO_2 gas, which raises the sensitivity of gas sensors (25).

The response and recovery time of nano ferrite Zn-$CdFe_2O_4/SnO_{2(0.15)}$ exposed to NO_2 gas are displayed in **Table (4).** Sample $Zn_{0.5}Cd_{0.5}Fe_2O_4/SnO_{2(0.15)}$ had the shortest response time (15.3 sec), and sample $ZnFe_2O_4/SnO_{2(0.15)}$ had the shortest recovery time (49.5 sec). This is because of the sol-gel process and its significant advantages, which include increased homogeneity, high purity, more uniform phase distributions in multi-component systems, and the potential to create novel nanophases (26).

Table 4. Minimum response and recovery time for Zn-$CdFe_2O_4$ / $SnO_{2(0.15)}$ samples to NO_2 gas.

Samples	Minimum response Time (s)	Operating Temperature (°C)	Minimum recovery Time (s)	Operating Temperature (°C)
M_1	19.8	250°C	49.5	300°C
M_2	16.2	200°C	54	250°C-300°C
M_3	15.3	300°C	62.1	250°C

3.5. Magnetic properties:

Figure (7) displayed the magnetic hysteresis ring, size, and shape of each of the Zn-$CdFe_2O_4$/$SnO_{2(0.15)}$ sample's ferrite nanoparticles as determined by the vibration magnetic device (VSM)

The composition of ferrite is the other factor that affects the rate at which cations diffuse in the solid state during sintering (27). To react to gases, ferrite sensors need to be thermally excited. The best response and recovery time is obtained at the optimum operating temperature 300°C (**Figure 6**). **Table (4)** demonstrates that samples of the produced compound had a minimum response time for NO_2 gas at operating temperature (300°C) and a minimum recovery time at operating temperature (300)°C.

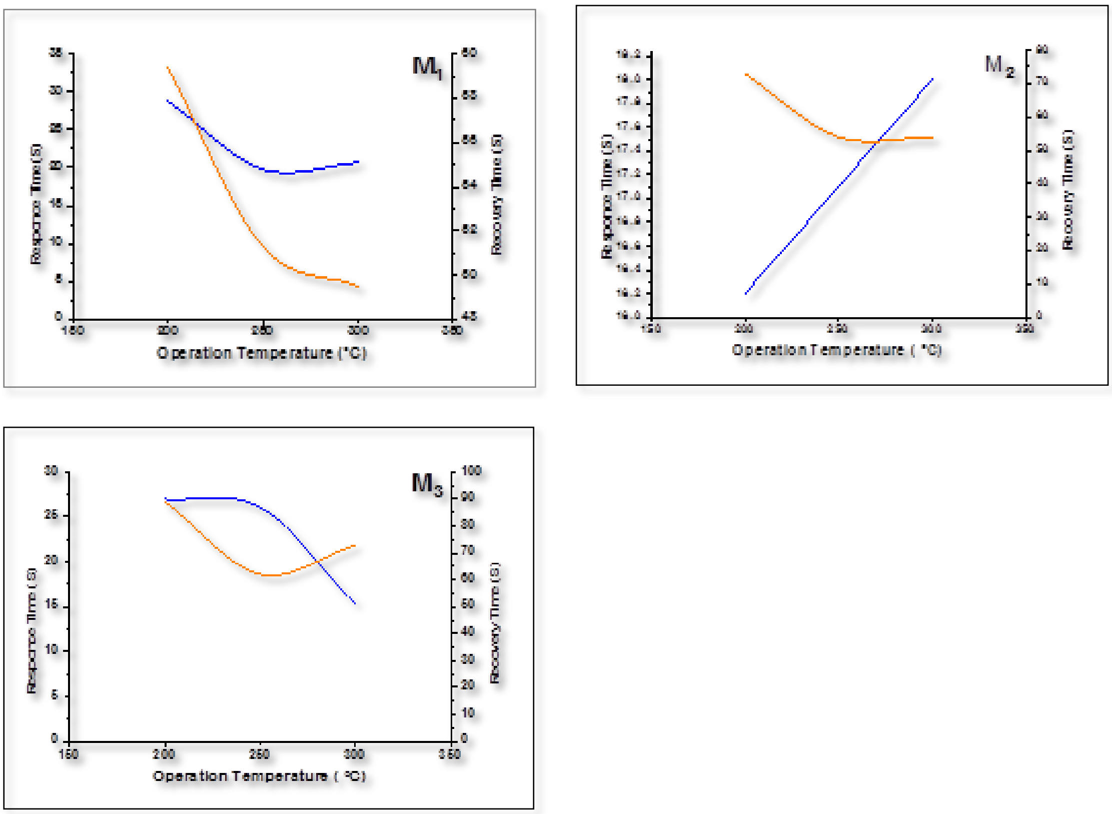

Figure 6. Relationship of recovery time and response time of NO_2 gas at operating temperature of Zn-$CdFe_2O_4$/$SnO_{2(0.15)}$ samples, where the blue line indicates response time, while the red line indicates recovery time.

The illustration (magnetic hysteresis loops) of nano ferrite is shown in **Figure (7).** Because of its tiny size, it has a soft magnetic nature. The tiny crystal size was demonstrated by examining XRD in **Table 2** (28), where earlier research verified that super magnetism is displayed by nanoparticles with a size less than 30nm or less than the critical size of the magnetic field (29, 30), The small and narrow hysteresis ring size significantly influenced by magnetic characteristics. Shape and width of the hysterical loop are influenced by the chemical content (31). The findings show that the magnetic characteristics of ferrite are altered by variations in the concentration of zinc and cadmium (32).

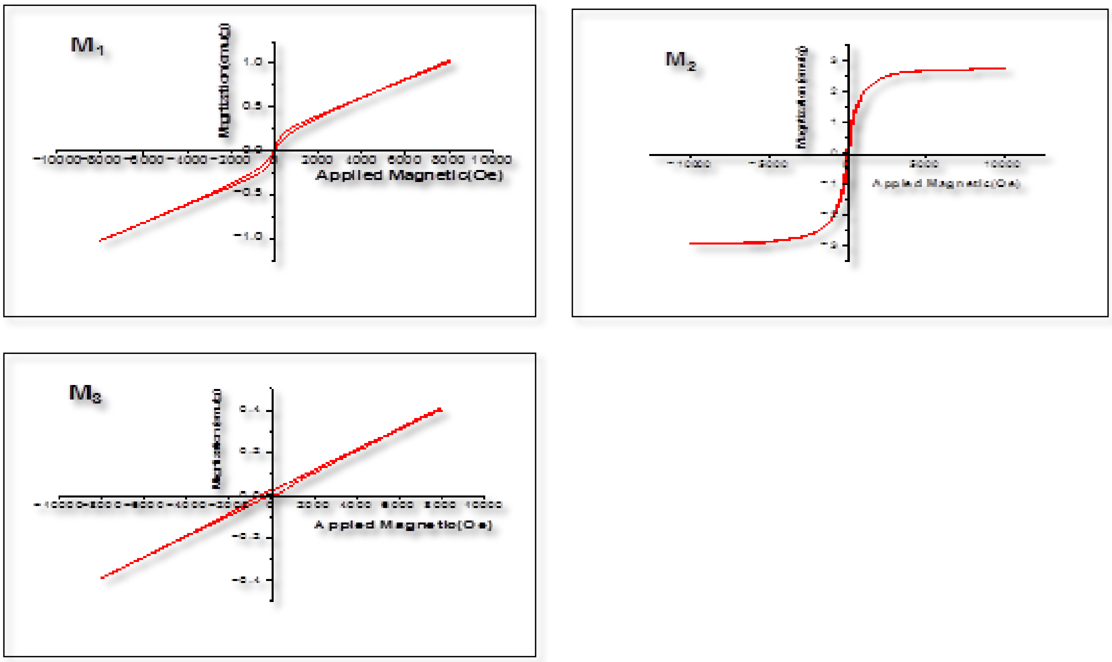

Figure 7. The relationship between magnetism and the applied field of Zn-$CdFe_2O_4/SnO_{2(0.15)}$.

Cd Ferrite is a strong contender for use as soft magnets and low-loss materials at high frequencies due to its outstanding electromagnetic performance, exceptional chemical stability, low coercive force, and mild saturation magnetization (33). Zinc causes lower crystalline magnetic anisotropy compared to Cd (17). Tiny may be added to samples to increase their magnetic (34) since SnO_2 is an n-type semiconductor with a wide energy gap Eg=3.6 eV (35) since the nanoparticles functioned as monopole particles causing a coherent spin magnetization reversal(36), because of variation in the lattice site configurations, crystal structures, particle compositions, and sizes the computed differences between Ms, Mr, and Hc (37, 38). Hc is the lowest for the $ZnFe_2O_4/SnO_{2(0.15)}$ and greatest for $Zn_{0.5}Cd_{0.5}Fe_2O_4/SnO_{2(0.15)}$ has Zn/Cd ratio 50/50, this is consistent with researchers' findings (17).

Table 5. Magnetic factor variation for $ZnCdFe_2O_4/SnO_{2(0.15)}$ nanoparticles.

Compound	Ms(emu/g)	Mr(emu/g)	Hc (Oe)
$ZnFe_2O_4/SnO_{2(0.15)}$	1.02	0.04	17.10
$CdFe_2O_4/SnO_{2(0.15)}$	2.71	0.47	60.54
$Zn_{0.5}Cd_{0.5}Fe_2O_4/SnO_{2(0.15)}$	0.41	0.02	610.39

4. Conclusion

Sol-gel synthesis was used to create Zn-$CdFe_2O_4/SnO_{2(0.15)}$ nano ferrite. The lattice constant of the sample $CdFe_2O_4/SnO_{2(0.15)}$ was higher than of the sample $ZnFe_2O_4/SnO_{2(0.15)}$, $Zn_{0.5}Cd_{0.5}Fe_2O_4/SnO_{2(0.15)}$, according to x-ray diffraction. Using Scherrer and Williamson-Hall analysis, we determined the grain size. The semi-spherical or spherical grains with some clusters and gaps in the scanning electron microscope (FE-SEM) pictures indicate the compound's nature and improve the sensor's responsiveness to gas. The sample recorded the highest sensitivity at the operating temperature of 250°C and the shortest response and recovery time at the temperature of 300°C. The nano ferrite exhibits good sensitivity to NO_2

at various temperatures. Using a hysteresis loop, the generated sample's soft magnetic nature was verified, where the results showed the Hc value was the highest for the sample $Zn_{0.5}Cd_{0.5}Fe_2O_4/SnO_2(0.15)$.

Acknowledgment

I would like to thank the staff of the Physics Department, Deanship of the College of Education for Pure Science (Ibn Al-Haitham), for their support in writing this research.

Conflict of Interest

The authors declare that they have no conflicts of interest.

Funding

None.

References

1. Rossinyol E, Arbiol J, Peiró F, Cornet A, Morante JR, Tian B, Bo T, Zhao D. Nanostructured metal oxides synthesized by hard template method for gas sensing applications. *Sens Actuators B Chem* 2005;109(1):57–63. https://doi.org/10.1016/j.snb.2005.03.016
2. Kadhim GA, Mohammed MA. Effect of the chloroform as a chemical treatment on gas sensing for cupcts/alq3 thin films. *Dig J Nanomater Biostruct* 2021;16(1).
3. Lassoued A, Lassoued MS, Karolak F, García-Granda S, Dkhil B, Ammar S, Gadri A. Synthesis, structural, optical, morphological and magnetic characterization of copper substituted nickel ferrite (CuxNi1−xFe2O4) through co-precipitation method. *J Mater Sci Mater Electron* 2017;28:18480–8. https://doi.org/10.1007/s10854-017-7795-4
4. Dey B, Bououdina M, Dhamodharan P, AsathBahadur S, Venkateshwarlu M, Manoharan C. Tuning the gas sensing properties of spinel ferrite NiFe2O4 nanoparticles by Cu doping. *J Alloys Compd* 2024;970:172711. https://doi.org/10.1016/j.jallcom.2023.172711
5. Pathak TK, Vasoya NH, Lakhani VK, Modi KB. Structural and magnetic phase evolution study on needle-shaped nanoparticles of magnesium ferrite. *Ceram Int* 2010;36(1):275–81. https://doi.org/10.1016/j.ceramint.2009.07.023
6. Kadu AV, Jagtap SV, Chaudhari GN. Studies on the preparation and ethanol gas sensing properties of spinel Zn0.6Mn0.4Fe2O4 nanomaterials. *Curr Appl Phys* 2009;9(6):1246–51. https://doi.org/10.1016/j.cap.2009.02.001
7. Nathani H, Gubbala S, Misra RD. Magnetic behavior of nanocrystalline nickel ferrite: Part I. The effect of surface roughness. *Mater Sci Eng B* 2005;121(1–2):126–36. https://doi.org/10.1016/j.mseb.2005.03.016
8. Anantharaman MR, Jagatheesan S, Malini KA, Sindhu S, Narayanasamy A, Chinnasamy CN, Jacobs JP, Reijne S, Seshan K, Smits RH, Brongersma HH. On the magnetic properties of ultra-fine zinc ferrites. *J Magn Magn Mater* 1998;189(1):83–8. https://doi.org/10.1016/S0304-8853(98)00171-1
9. Shenoy SD, Joy PA, Anantharaman MR. Effect of mechanical milling on the structural, magnetic and dielectric properties of coprecipitated ultrafine zinc ferrite. *J Magn Magn Mater* 2004;269(2):217–26. https://doi.org/10.1016/S0304-8853(03)00596-1
10. Mehrfar SK, Fallah Shojaei A, Moradi–Shoeili Z. Performance evaluation of gas sensors based on spinel ferrites MFe2O4 (M= Cd, Co, Zn) for detecting the linalool. *Inorg Nano-Met Chem* 2023:1–9. https://doi.org/10.1080/24701556.2023.2271453
11. Rezlescu N, Rezlescu E, Tudorache F, Popa PD. Gas sensing properties of porous Cu-, Cd- and Zn-ferrites. *Rom Rep Phys* 2009;61(2):223–34.
12. Mostafa M, Salem BI. Studying structural, molecular, morphological and electrical properties of Co0.2Zn0.8Fe2O4 doped with Cadmium. *Mater Sci Eng B* 2022;286:116043. https://doi.org/10.1016/j.mseb.2022.116043

13. Kadhim SA, Al-Saadi TM. Study of the effect of Ce3+ on the gas sensitivity and magnetic properties of CuxCe0.3-xNi0.7Fe2O4 ferrite nanoparticles. *Mater Sci Forum* 2023;1083:3–12. https://doi.org/10.4028/p-tw92h3
14. Al-Saadi TM, Kadhim SA. Preparation and study some properties of ferrite nanoparticles (CuxAl0.3-xNi0.7Fe2O4). *Iraqi J Sci* 2024;65(7):3765–75. https://doi.org/10.24996/ijs.2024.65.7.17
15. Al-Saadi TM, Alsaady LJ. Preparation of silver nanoparticles by sol-gel method and study their characteristics. *Ibn Al-Haitham J Pure Appl Sci* 2015;28(1):301–10. https://jih.uobaghdad.edu.iq/index.php/j/article/view/214
16. Benrabaa R, Löfberg A, Rubbens A, Bordes-Richard E, Vannier RN, Barama A. Structure, reactivity and catalytic properties of nanoparticles of nickel ferrite in the dry reforming of methane. *Catal Today* 2013;203:188–95. https://doi.org/10.1016/j.cattod.2012.06.002
17. Tanveer M, Nisa I, Nabi G, Hussain MK, Khalid S, Qadeer MA. Sol-gel extended hydrothermal pathway for novel Cd-Zn co-doped Mg-ferrite nano-structures and a systematic study of structural, optical and magnetic properties. *J Magn Magn Mater* 2022;553:169245. https://doi.org/10.1016/j.jmmm.2022.169245
18. Al-Saadi TM, Kamil ZA. Study the effect of manganese ion doping on the size-strain of SnO2 nanoparticles using X-ray diffraction data. *Ibn Al-Haitham J Pure Appl Sci* 2023;36(3):158–66. https://doi.org/10.30526/36.3.3052
19. Mahdi HI, Al-Saadi TM, Bakr NA. Fabrication and characterization of CoxMn0.25−xMg0.75Fe2O4 nanoparticles for H2S sensing applications. *J Mater Sci Mater Electron* 2023;34(22):1634. https://doi.org/10.1007/s10854-023-11064-8
20. Ahmad D, Ali A, Abbas Z, Zaman A, Alsuhaibani AM, Tirth V, Sarker MR, Kamari NA, Algahtani A, Aljohani M. Structural, optical and dielectric properties of holmium-doped nickel-cadmium ferrite nanoparticles synthesized by sol-gel auto-combustion method. *Crystals* 2023;13(3):495. https://doi.org/10.3390/cryst13030495
21. Muslim T, Kadhim SA. The gas sensitivity properties of nano ferrite CuxAl0.3−xNi0.7Fe2O4 synthesized by sol-gel method. *Ibn Al-Haitham J Pure Appl Sci* 2023;36(4):159–70. https://doi.org/10.30526/36.4.3118
22. Al-Saadi TM, Abed AH, Salih AA. Synthesis and characterization of AlyCu0.15Zn0.85−yFe2O4 ferrite prepared by the sol-gel method. *Int J Electrochem Sci* 2018;13(9):8295–302. https://doi.org/10.20964/2018.09.04
23. Saheb L, Al-Saadi TM. Synthesis, characterization, and NH3 sensing properties of (Zn0.7Mn0.3−xCexFe2O4) nano-ferrite. *J Phys Conf Ser* 2021;2114(1):012040. https://doi.org/10.1088/1742-6596/2114/1/012040
24. Li Y, Wang Z, Liu R. Superparamagnetic α-Fe2O3/Fe3O4 heterogeneous nanoparticles with enhanced biocompatibility. *Nanomaterials* 2021;11(4):834. https://doi.org/10.3390/nano11040834
25. Manikandan V, Sikarwar S, Yadav BC, Mane RS. Fabrication of tin substituted nickel ferrite (Sn-NiFe2O4) thin film and its application as opto-electronic humidity sensor. *Sens Actuators A Phys* 2018;272:267–73. https://doi.org/10.1016/j.sna.2018.01.059
26. Sankaranarayanan R, Shailajha S, Dineshkumar C. Investigation on structural and H2 gas sensing response of AlCdZnNiFe2O4 sensor material. *Ceram Int* 2022;48(1):720–31. https://doi.org/10.1016/j.ceramint.2021.09.152
27. Tudorache F, Rezlescu E, Popa PD, Rezlescu N. Study of some simple ferrites as reducing gas sensors. *J Optoelectron Adv Mater* 2008;10:1889–93.
28. Mahdi HI, Bakr NA, Al-Saadi TM. Studying the gas sensitivity and magnetic properties of magnesium ferrite prepared by the sol-gel route. *Iraqi J Sci* 2024;65(8):4313–24. https://doi.org/10.24996/ijs.2024.65.8.16
29. Carlos L, Einschlag FS, González MC, Mártire DO. Applications of magnetite nanoparticles for heavy metal removal from wastewater. *Waste Water Treat Technol Recent Anal Dev* 2013;3:64–73. https://doi.org/10.5772/54608

30. Mascolo M, Pei Y, Ring T A. Room temperature co-precipitation synthesis of magnetite nanoparticles in a large pH window with different bases. Materials. 2014;6(12):5549–5567. https://doi.org/10.3390/ma6125549
31. Hadi K, Al-Saadi T M. Investigating the structural and magnetic properties of nickel oxide nanoparticles prepared by precipitation method. Ibn Al-Haitham J Pure Appl Sci. 2022;35(4):94–103. https://doi.org/10.30526/35.4.2872
32. Kaur H, Singh A, Kumar V, Ahlawat D S. Structural, thermal and magnetic investigations of cobalt ferrite doped with Zn^{2+} and Cd^{2+} synthesized by auto combustion method. J Magn Magn Mater. 2019;474:505–511. https://doi.org/10.1016/j.jmmm.2018.11.010
33. Naseri M. Optical and magnetic properties of monophasic cadmium ferrite ($CdFe_2O_4$) nanostructure prepared by thermal treatment method. J Magn Magn Mater. 2015;392:107–113. https://doi.org/10.1016/j.jmmm.2015.05.026
34. Kiani M, Tian X Q, Kiani A B, ur Rehman S, Khan S A, Khan K, Tareen A K, Khan Q U, Mahmood I. A first principal study: effect of tin substitution on magnetic properties of bismuth ferrite nanoparticles prepared by sol–gel synthesis method. Inorg Chem Commun. 2021;127:108483. https://doi.org/10.1016/j.inoche.2021.108483
35. Aegerter M A, Reich A, Ganz D, Gasparro G, Pütz J, Krajewski T. Comparative study of SnO_2: Sb transparent conducting films produced by various coating and heat treatment techniques. J Non-Cryst Solids. 1997;218:123–128. https://doi.org/10.1016/S0022-3093(97)00134-8
36. Wang F, Lakhtakia A (eds). Selected papers on nanotechnology: theory and modeling. Spie Press. 2006.
37. Abdallah H M, Moyo T, Ngema N. The effect of temperature on the structure and magnetic properties of $Co_{0.5}Ni_{0.5}Fe_2O_4$ spinel nanoferrite. J Magn Magn Mater. 2015;394:223–228. https://doi.org/10.1016/j.jmmm.2015.06.061
38. Köseoğlu Y. Structural, magnetic, electrical and dielectric properties of $Mn_xNi_{1-x}Fe_2O_4$ spinel nanoferrites prepared by PEG assisted hydrothermal method. Ceram Int. 2013;39(4):4221–4230. https://doi.org/10.1016/j.ceramint.2012.11.004